PHYSICAL REVIEW A **74**, 043420 (2006)

Configuration-interaction-based time-dependent orbital approach for *ab initio* treatment of electronic dynamics in a strong optical laser field

Nina Rohringer,[1] Ariel Gordon,[2] and Robin Santra[1]
[1]*Argonne National Laboratory, Argonne, Illinois 60439, USA*
[2]*Department of Electrical Engineering and Computer Science and Research Laboratory of Electronics, Massachusetts Institute of Technology, Cambridge, Massachusetts 02139, USA*

(Received 1 August 2006; published 30 October 2006)

The time-dependent configuration interaction singles (TDCIS) method—an *ab initio* electronic-structure technique with predictive character—is reformulated in terms of an effective one-electron theory with coupled channels. In this form, the TDCIS equations of motion may be evaluated using standard wave-packet propagation techniques in real space. The time-dependent orbital formulation of TDCIS has computational and conceptual advantages for studying strong-field phenomena in many-electron systems. A simplified version of this theory, referred to as the determinantal single-active-electron (d-SAE) method, is derived. TDCIS and d-SAE are tested by their application to a one-dimensional two-electron model in a strong laser field. The numerically exact time-dependent dipole moment of the interacting system is found to be very well reproduced with TDCIS. The d-SAE method is less accurate, but still provides superior performance in comparison to the standard single-active-electron approach.

DOI: 10.1103/PhysRevA.74.043420 PACS number(s): 32.80.Rm, 31.25.−v, 42.65.Ky, 31.15.Ar

I. INTRODUCTION

At optical wavelengths, typical molecules and many atoms cannot be electronically excited by the absorption of a single photon. When the optical radiation field is made sufficiently intense, however, multiphoton absorption can take place and there is an observable electronic response. Among the interesting phenomena associated with the optical strong-field excitation of atoms and molecules is the generation of high-order harmonics (HHG) of the driving laser frequency [1–3]. The high-order harmonics may serve as a convenient source of coherent XUV and soft x-ray radiation [4–8]. HHG technology forms the basis for the production of attosecond pulses [9,10]. HHG can be utilized to study the properties of atoms and molecules in an ultrafast manner [11–15]. The last application, in particular, which focuses somewhat less on the optical physics than on the atomic and molecular physics underlying HHG, requires the support by a reliable and practically feasible electronic structure theory to unlock the full potential of the HHG approach. The interpretation of experimental data only in terms of the three-step model [16–18] can be problematic [19–22] and seems to impose an unnecessary limitation.

Clearly, the most accurate way to describe the physics of an atom or molecule interacting with a strong laser pulse is to solve the exact time-dependent Schrödinger equation for the system. The problem is that in the many-electron case, this is not practically feasible. The usual strategy adopted at this point is to recall one key concept of the three-step model: the assumption that there is only a single active electron contributing to the HHG process. The standard single-active-electron (s-SAE) approach consists in the solution of an effective one-particle Schrödinger equation [23–29]

$$i\frac{\partial}{\partial t}\psi(\mathbf{x},t) = \left(-\frac{1}{2}\nabla^2 + V_{\mathrm{SAE}}(\mathbf{x}) - \mathcal{E}(t)z\right)\psi(\mathbf{x},t) \tag{1}$$

for the one-particle orbital $\psi(\mathbf{x},t)$. (Atomic units are used throughout.) The single electron is assumed to move in a suitably chosen potential $V_{\mathrm{SAE}}(\mathbf{x})$. (Potentials commonly employed are local and time-independent.) The system is exposed to a linearly polarized laser field of strength $\mathcal{E}(t)$ (polarization along the z axis). Within the s-SAE approach, the expectation value of, for example, the electric-dipole operator along the z axis is approximated by

$$\langle z\rangle = \langle \psi,t|z|\psi,t\rangle . \tag{2}$$

While s-SAE is attractive due to its simplicity, it lacks any formal justification. It cannot be derived from first principles. More rigorous effective one-electron approaches to the strong-field problem are time-dependent Hartree-Fock (TDHF) [30,31] and time-dependent density-functional theory (TDDFT) in the Kohn-Sham formulation [32,33]. However, there are well-known problems with TDHF [34–36]; practical TDDFT calculations are affected by similar limitations [37,38]. More reliable, but computationally much more challenging than an effective one-electron method is the recently developed multiconfiguration time-dependent Hartree-Fock method [39,40].

Less explored, in the context of strong-field physics, is the method of configuration interaction (CI) [41]. Computationally and conceptually attractive is the CI singles (CIS) approach [42,43], which is variational, size-consistent, and applicable to large molecules. Its time-dependent version, TDCIS, has recently been applied to inelastic electron scattering within a one-dimensional jellium model [44] and to the laser-induced excitation of a polyatomic molecule [45]. In the latter application, the laser intensity did not exceed 10^{12} W/cm^2, so that strong-field ionization could be neglected. References [44,45] adopt the following strategy. In a first step, eigenstates of the many-body system are calculated using stationary CIS. The time-dependent many-body wave function is represented in this basis, and the equation of motion satisfied by the vector of CIS expansion coefficients is solved.

One of the purposes of this paper is to show that TDCIS can be written as an effective one-electron theory with coupled channels. We present in Sec. II A a time-dependent orbital formulation of TDCIS, which renders TDCIS calculations amenable to wave-packet propagation techniques in real space. For instance, there is no need to calculate the virtual orbitals of the chosen one-particle model. There is also no need to construct and diagonalize the CIS matrix. A second purpose is to develop a simple scheme to improve on the s-SAE equations. This is discussed in Sec. II B. In Sec. III, we present a numerical application to a one-dimensional two-electron system in a strong laser field. (In the calculations, the Keldysh parameter is about one.) This allows us to assess the quality of the effective one-electron techniques discussed in Secs. II A and II B. Conclusions are drawn in Sec. IV.

II. DERIVATION OF EFFECTIVE ONE-ELECTRON APPROACHES FROM TDCIS

The following derivation focuses on atoms or molecules with a closed-shell ground state. (The vast majority of stable molecules fall into this category.) Let $|\varphi_{p\sigma}\rangle$ stand for the eigenstates (spin orbitals) of the selected one-particle Hamiltonian $\hat{H}_0$ (p is the spatial index, σ is the spin label). In the language of second quantization [46,47], the noninteracting ground state of an N-electron closed-shell system may be written as

$$|\Phi_0\rangle = \prod_{i=1}^{N/2} \hat{c}_{i-}^{\dagger}\hat{c}_{i+}^{\dagger}|0\rangle, \tag{3}$$

where $|0\rangle$ is the vacuum state and $\hat{c}_{p\sigma}^{\dagger}$ creates an electron in spin orbital $|\varphi_{p\sigma}\rangle$, i.e., $\hat{c}_{p\sigma}^{\dagger}|0\rangle = |\varphi_{p\sigma}\rangle$. The one-particle Hamiltonian in the absence of the laser field reads

$$\hat{H}_0 = \sum_p \varepsilon_p \sum_\sigma \hat{c}_{p\sigma}^{\dagger}\hat{c}_{p\sigma}, \tag{4}$$

such that

$$\hat{H}_0|\varphi_{p\sigma}\rangle = \varepsilon_p|\varphi_{p\sigma}\rangle. \tag{5}$$

The ε_p are the orbital energies.

Using the spin orbitals $|\varphi_{p\sigma}\rangle$, a set of N-electron determinants can be formed that may serve as a basis to represent the exact eigenstates (and, therefore, arbitrary wave packets) of the interacting N-electron system. Determining the exact Hamiltonian in this basis and diagonalizing the resulting matrix is known as the method of CI [41]. A systematic way to construct the basis states is to start with $|\Phi_0\rangle$ and then remove one electron from an occupied orbital in $|\Phi_0\rangle$ and replace it with an electron in an orbital that is unoccupied in the noninteracting ground state. In this way, the class of singly-excited (or particle-hole) configurations is obtained. Adding all higher (double, triple, etc.) excitation classes allows one to generate a complete basis for the N-electron problem, provided the orbital basis is complete. While this procedure is formally rigorous, it is in general not practical: The order of CI matrices increases rapidly with the number of excitation classes included.

In the following, we restrict our analysis to $|\Phi_0\rangle$ and its single excitations (CIS). We will exploit that at the CIS level, if and only if $\hat{H}_0$ is the Fock operator associated with the Hartree-Fock ground state of the N-electron system, the exact, laser-free Hamiltonian does not couple $|\Phi_0\rangle$ to any of the single excitations (Brillouin theorem) [41]. Within CIS, the Hartree-Fock ground state remains stationary in the absence of an external perturbation. Choosing $\hat{H}_0$ as the N-electron Fock operator has practical and conceptual advantages. First, all equations derived from the CIS matrix elements will be as compact as possible. Second, excitations out of occupied orbitals occur only as a consequence of the interaction with a laser pulse, not due to electron-electron interactions. If another single-particle model (i.e., another $\hat{H}_0$) were selected, the CIS ground state would have particle-hole components. The laser field could couple these directly to doubly excited configurations.

Let us now consider the behavior of the N-electron system under the influence of a linearly polarized laser field. Neglecting laser magnetic field effects and relativistic effects such as spin-orbit coupling, the total spin ($S=0$) is a conserved quantity. Thus, in the framework of TDCIS, the many-body wave packet is given by

$$|\Psi,t\rangle = \alpha_0(t)|\Phi_0\rangle + \sum_i \sum_a \alpha_i^a(t)|\Phi_i^a\rangle, \tag{6}$$

where

$$|\Phi_i^a\rangle = \frac{1}{\sqrt{2}}\{\hat{c}_{a+}^{\dagger}\hat{c}_{i+} + \hat{c}_{a-}^{\dagger}\hat{c}_{i-}\}|\Phi_0\rangle. \tag{7}$$

Here and in the following, indices $i,j,k,l,\ldots$ are used for spatial orbitals that are doubly occupied in $|\Phi_0\rangle$. Unoccupied (virtual) orbitals are symbolized by indices $a,b,c,d,\ldots$, whereas for general orbitals (occupied or unoccupied) indices $p,q,r,s,\ldots$ are employed. In view of the discussion above, the expansion coefficients $\alpha_0(t)$ and $\alpha_i^a(t)$ may be chosen to satisfy the initial conditions (before the laser pulse)

$$\alpha_0(t \to -\infty) = 1, \tag{8}$$

$$\alpha_i^a(t \to -\infty) = 0. \tag{9}$$

Based on the TDCIS ansatz for the time-dependent wave function [Eq. (6)], different hierarchies of effective one-electron approaches can be derived.

A. Orbital formulation of TDCIS: Exact Hamiltonian

In the following, we reformulate TDCIS in terms of a set of coupled equations for time-dependent orbitals (single-particle wave functions). The one-body Hamiltonian $\hat{H}_0$ defining the orbitals used in the TDCIS expansion is fixed as the Fock operator of the Hartree-Fock ground state. In other words, the TDCIS expansion in Eq. (6) is based on the occupied and virtual Hartree-Fock ground-state orbitals.

Let the N-electron system be subject to a laser field [field strength $\mathcal{E}(t)$] linearly polarized along the z axis. Within the electric-dipole approximation, the time-dependent many-body Hamiltonian can be written as

$$\hat{H}(t) = \hat{H}_0 + \hat{H}_1 - E_0^{(\mathrm{HF})} - \mathcal{E}(t)\hat{z}, \tag{10}$$

where

$$\hat{H}_1 = \hat{V}^{\mathrm{C}} - \hat{V}^{(\mathrm{HF})}, \tag{11}$$

$$\hat{V}^{\mathrm{C}} = \frac{1}{2}\sum_{p\sigma_p q\sigma_q r\sigma_r s\sigma_s} v_{p\sigma_p q\sigma_q r\sigma_r s\sigma_s}\hat{c}^{\dagger}_{p\sigma_p}\hat{c}^{\dagger}_{q\sigma_q}\hat{c}_{s\sigma_s}\hat{c}_{r\sigma_r} \tag{12}$$

is the Coulomb two-body operator, and

$$\hat{V}^{(\mathrm{HF})} = \sum_{p\sigma_p q\sigma_q}\left\{\sum_{i\sigma_i} v_{p\sigma_p, i\sigma_i[q\sigma_q, i\sigma_i]}\right\}\hat{c}^{\dagger}_{p\sigma_p}\hat{c}_{q\sigma_q} \tag{13}$$

represents the interaction with the Hartree-Fock mean-field ($v_{p\sigma_p,q\sigma_q[r\sigma_r,s\sigma_s]}=v_{p\sigma_p q\sigma_q r\sigma_r s\sigma_s}-v_{p\sigma_p q\sigma_q s\sigma_s r\sigma_r}$). Note that

$$v_{p\sigma_p q\sigma_q r\sigma_r s\sigma_s} = v_{pqrs}\delta_{\sigma_p\sigma_r}\delta_{\sigma_q\sigma_s}. \tag{14}$$

In this expression, and in the remainder of the paper, all electron-electron interaction matrix elements

$$v_{pqrs} = \int\int d^3x_1 d^3x_2 \varphi_p^*(\mathbf{x}_1)\varphi_q^*(\mathbf{x}_2) r_{12}^{-1}\varphi_r(\mathbf{x}_1)\varphi_s(\mathbf{x}_2) \tag{15}$$

refer to spatial orbitals.

In Eq. (10) a constant energy shift has been introduced to render subsequent equations more compact. The energy shift is chosen as the Hartree-Fock ground-state energy

$$E_0^{(\mathrm{HF})} = 2\sum_i \varepsilon_i + \langle\Phi_0|\hat{H}_1|\Phi_0\rangle, \tag{16}$$

where

$$\langle\Phi_0|\hat{H}_1|\Phi_0\rangle = -\sum_{ij}\{2v_{ijij} - v_{ijji}\}. \tag{17}$$

The remaining matrix elements of $\hat{H}_1$, which within CIS describe electron-correlation effects, are determined using the Slater-Condon rules [41]

$$\langle\Phi_0|\hat{H}_1|\Phi_i^a\rangle = 0 \quad \text{(Brillouin theorem)}, \tag{18}$$

$$\langle\Phi_i^a|\hat{H}_1|\Phi_{i'}^{a'}\rangle = 2v_{ai'ia'} - v_{ai'a'i} + \delta_{ii'}\delta_{aa'}\langle\Phi_0|\hat{H}_1|\Phi_0\rangle. \tag{19}$$

The dipole operator, shown here in the length form, is a one-body operator,

$$\hat{z} = \sum_{pq} z_{pq}\sum_{\sigma}\hat{c}^{\dagger}_{p\sigma}\hat{c}_{q\sigma}, \tag{20}$$

where the dipole matrix elements in terms of spatial orbitals are defined as

$$z_{pq} = \int d^3x\,\varphi_p^*(\mathbf{x}) z \varphi_q(\mathbf{x}). \tag{21}$$

The matrix elements of $\hat{z}$ with respect to the many-electron basis vectors employed to expand the wave packet are

$$\langle\Phi_0|\hat{z}|\Phi_0\rangle = 2\sum_i z_{ii}, \tag{22}$$

$$\langle\Phi_0|\hat{z}|\Phi_i^a\rangle = \sqrt{2}z_{ia}, \tag{23}$$

$$\langle\Phi_i^a|\hat{z}|\Phi_{i'}^{a'}\rangle = \delta_{ii'}z_{aa'} - \delta_{aa'}z_{i'i} + \delta_{ii'}\delta_{aa'}2\sum_j z_{jj}. \tag{24}$$

The diagonal dipole terms z_{ii} and z_{aa} vanish for atomic systems and are omitted in the following (i.e., $z_{ii}=0$ and $z_{aa}=0$ throughout).

Inserting the ansatz (6) into the time-dependent Schrödinger equation,

$$i\frac{\partial}{\partial t}|\Psi,t\rangle = \hat{H}(t)|\Psi,t\rangle, \tag{25}$$

and projecting the resulting expression onto $|\Phi_0\rangle$ and $|\Phi_i^a\rangle$, respectively, the equations of motion for the expansion coefficients α_0 and α_i^a can be derived;

$$i\dot{\alpha}_0 = -\sqrt{2}\mathcal{E}(t)\sum_i\sum_a \alpha_i^a z_{ia}, \tag{26}$$

$$\begin{aligned} i\dot{\alpha}_i^a = {}& (\varepsilon_a - \varepsilon_i)\alpha_i^a + \sum_{i'}\sum_{a'}\alpha_{i'}^{a'}(2v_{ai'ia'} - v_{ai'a'i}) - \mathcal{E}(t) \\ & \times\left\{\sqrt{2}\alpha_0 z_{ai} + \sum_{a'}\alpha_i^{a'}z_{aa'} - \sum_{i'}\alpha_{i'}^a z_{i'i}\right\}. \end{aligned} \tag{27}$$

As is generally the case when the Hilbert space is truncated, the TDCIS equations are, strictly speaking, not gauge invariant. Transforming the Schrödinger equation in the CIS subspace from length gauge to velocity gauge would lead to couplings to higher-excited configurations. Solving Eqs. (26) and (27) in the velocity gauge would therefore give slightly different results.

We note that the direct Coulomb matrix elements $v_{ai'a'i}$ and the exchange matrix elements $v_{ai'ia'}$ can be written as

$$v_{ai'a'i} =: \langle\varphi_a|\hat{J}_{i'i}|\varphi_{a'}\rangle, \tag{28}$$

$$v_{ai'ia'} =: \langle\varphi_a|\hat{K}_{i'i}|\varphi_{a'}\rangle, \tag{29}$$

where $\hat{J}_{i'i}$ and $\hat{K}_{i'i}$ are, respectively, generalized Coulomb and exchange operators associated with the orbitals $|\varphi_i\rangle$ and $|\varphi_{i'}\rangle$. The equations of motion (26) and (27) may now be recast in terms of a coupled set of effective one-particle Schrödinger equations. For this purpose, we introduce a time-dependent orbital that collects all the single excitations originating from the occupied orbital $|\varphi_i\rangle$,

$$|\chi_i,t\rangle = \frac{1}{\sqrt{2}}\sum_a \alpha_i^a(t)|\varphi_a\rangle. \tag{30}$$

The orbitals $|\chi_i,t\rangle$ satisfy the initial condition [cf. Eq. (9)]

$$|\chi_i, t\rightarrow -\infty\rangle = 0 \tag{31}$$

and are, for all t, orthogonal to all orbitals occupied in the Hartree-Fock ground state. [The factor of $1/\sqrt{2}$ in Eq. (30) is purely cosmetic.] Using Eq. (27) and the definition

$$\hat{P} = \sum_a |\varphi_a\rangle\langle\varphi_a| = \mathbb{I} - \sum_i |\varphi_i\rangle\langle\varphi_i|, \tag{32}$$

the equation of motion satisfied by $|\chi_i,t\rangle$ reads

$$i\frac{\partial}{\partial t}|\chi_i\rangle = (\hat{H}_0 - \varepsilon_i)|\chi_i\rangle + \sum_{i'} \hat{P}\{2\hat{K}_{i'i} - \hat{J}_{i'i}\}|\chi_{i'}\rangle - \mathcal{E}(t)\hat{P}\hat{z}\{\alpha_0|\varphi_i\rangle + |\chi_i\rangle\} + \mathcal{E}(t)\sum_{i'} z_{i'i}|\chi_{i'}\rangle. \tag{33}$$

This establishes a system of linear, coupled one-particle equations for the orbitals $|\chi_i\rangle$. These equations describe the time evolution of the $|\chi_i\rangle$, which become populated (i.e., their norm increases) over time under the action of the laser field. Populating $|\chi_i\rangle$ corresponds to exciting an electron out of $|\varphi_i\rangle$.

We would like to point out that TDCIS properly accounts for Coulomb-mediated couplings among the particle-hole configurations $|\Phi_i^a\rangle$. In other words, whereas the long-range potential associated with the Fock operator $\hat{H}_0$ is that of a neutral system [41] (assuming that the N-electron system is neutral), the operators $2\hat{K}_{i'i} - \hat{J}_{i'i}$ in Eq. (33) ensure that the excited electron experiences a Coulomb attraction to the residual cation. Exploiting the orthogonality among the orbitals $|\varphi_i\rangle$, it may be shown that for large distances of the electron from the cation

$$\sum_{i'} \langle \mathbf{x}|\hat{P}\{2\hat{K}_{i'i} - \hat{J}_{i'i}\}|\chi_{i'}\rangle = -\frac{1}{|\mathbf{x}|}\chi_i(\mathbf{x},t) + O\left(\frac{1}{|\mathbf{x}|^2}\right). \tag{34}$$

Also note that in the formalism adopted here, the ionization potential I_i (corresponding to the formation of a hole in orbital $|\varphi_i\rangle$) is given by $-\varepsilon_i$ (Koopmans' theorem [48]). For outer-valence shells, Koopmans' theorem is typically accurate to within the energy of an optical photon [49,50]. For strong-field applications, this may not be sufficiently accurate. Since $-\varepsilon_i$ enters Eq. (33) as a parameter, it may simply be replaced, if necessary, with the experimentally determined I_i.

With the definition given in Eq. (30), the equation of motion for the ground-state amplitude α_0 [Eq. (26)] simplifies to

$$i\dot{\alpha}_0 = -2\mathcal{E}(t)\sum_i \langle\varphi_i|\hat{z}|\chi_i,t\rangle. \tag{35}$$

By calculating α_0 and the $|\chi_i\rangle$'s from Eqs. (33) and (35), all information is obtained to determine, for example, the TDCIS expectation value of an arbitrary spin-independent one-body operator $\hat{D} = \Sigma_{pq} d_{pq} \Sigma_\sigma c^\dagger_{p\sigma} c_{q\sigma}$;

$$\langle\Psi,t|\hat{D}|\Psi,t\rangle = 2|\alpha_0|^2 \sum_i d_{ii} + 2\sum_i \langle\chi_i,t|\hat{d}|\chi_i,t\rangle + 4\sum_i d_{ii}\sum_j \langle\chi_j,t|\chi_j,t\rangle - 2\sum_{ii'} d_{ii'}\langle\chi_{i'},t|\chi_i,t\rangle + 4\,\mathrm{Re}\left(\alpha_0\sum_i \langle\chi_i,t|\hat{d}|\varphi_i\rangle\right). \tag{36}$$

Another quantity that is easily calculated within this framework is the reduced density matrix of the residual ion produced in the excitation (ionization) process. Let

$$\hat{\rho}(t) = |\Psi,t\rangle\langle\Psi,t| \tag{37}$$

denote the density operator of the N-electron system. The matrix elements of the reduced density matrix of the residual ion may then be defined as [51]

$$\rho^{(\mathrm{ion})}_{ii'}(t) := \sum_a \langle\Phi_i^a|\hat{\rho}(t)|\Phi_{i'}^a\rangle. \tag{38}$$

Hence, using Eqs. (6) and (37),

$$\rho^{(\mathrm{ion})}_{ii'}(t) = 2\langle\chi_{i'},t|\chi_i,t\rangle. \tag{39}$$

This can be used to explore whether—and to which degree—the strong-field ionization process establishes coherences among the one-hole ionization channels. With the help of Eqs. (30) and (39), the conservation of the norm of $|\Psi,t\rangle$ [Eq. (6)] can be expressed as

$$|\alpha_0(t)|^2 + \sum_i \rho^{(\mathrm{ion})}_{ii}(t) = 1. \tag{40}$$

Thus, $\rho^{(\mathrm{ion})}_{ii}(t)$ may be interpreted as the probability of forming a hole in orbital $|\varphi_i\rangle$.

The autocorrelation function $C(t)$ of the TDCIS many-body wave packet $|\Psi,t\rangle$ is another useful quantity that can be calculated from α_0 and the $|\chi_i\rangle$'s;

$$C(t) = \langle\Psi,t_0|\Psi,t\rangle = \alpha_0^*(t_0)\alpha_0(t) + 2\sum_i \langle\chi_i,t_0|\chi_i,t\rangle. \tag{41}$$

After the laser pulse, the many-body Hamiltonian $\hat{H}(t) = \hat{H}$ [Eq. (10)] is stationary. Therefore, assuming that the laser electric field $\mathcal{E}(t)$ vanishes for $t \geqslant t_0$, the spectral composition (including weights) of $|\Psi,t\rangle$ with respect to the eigenstates of $\hat{H}$ can be extracted from $C(t)$ [52,53]. For this purpose, one may utilize the filter diagonalization method [54,55], which is particularly powerful if, for practical reasons, $C(t)$ can be calculated for only a short time segment after t_0. In order to determine the photoelectron spectrum, Eq. (41) suggests one spectrally analyze the individual channel autocorrelation functions, $2\langle\chi_i,t_0|\chi_i,t\rangle$, and then subtract from each channel spectrum the corresponding channel energy, $-\varepsilon_i$. [Note that in view of Eq. (35), $\alpha_0(t) = \alpha_0(t_0)$.] This strategy gives the photoelectron spectrum associated with each individual channel, under the assumption that the channel couplings in the wave-packet propagation are weak. As Eq. (34) demonstrates, channel couplings drop at least as fast as $1/|\mathbf{x}|^2$, where $|\mathbf{x}|$ is the distance of the photoelectron from the parent ion. The total photoelectron spectrum is obtained as the sum over the channel spectra.

Our analysis shows that TDCIS can be reformulated as a time-dependent orbital approach. Neither the explicit calculation of the virtual HF orbitals $|\varphi_a\rangle$ (or matrix elements with respect to them) nor the calculation of the expansion coefficients $\alpha_i^a(t)$ is necessary to solve Eqs. (33) and (35). This is an advantage over the traditional formulation of TDCIS in the case of laser-driven systems, where ionization may play a key role. In processes like HHG, an accurate treatment of the continuum part of the wave function is crucial, i.e., a sizable number of continuum orbitals $|\varphi_a\rangle$ have to be explicitly calculated. This may render the conventional implementation of TDCIS inefficient. The time-dependent orbital approach circumvents this problem by potentially allowing one to employ the efficient grid methods and wave-packet propagation techniques that have been developed for quantum-dynamical problems (see, for example, Ref. [56]). Maybe more important is the fact that an effective orbital picture is ideally suited for direct visualization of the wave-packet dynamics. Finally, the computational effort to solve Eq. (33) together with Eq. (35) is comparable to a standard TDHF calculation with several active orbitals. However, as we will see in Sec. III, TDCIS may generally be expected to provide a superior description of electronic many-body physics in a laser field.

B. Approximate one-body Hamiltonian

Even if a simple one-body Hamiltonian is assumed, the TDCIS ansatz (6) predicts a dynamical behavior that differs from that obtained within the s-SAE approach. This is demonstrated in the following. In particular, we formulate an improved version of SAE theory that takes electron spin into account.

We assume that the dynamics of the N-electron system is governed by an appropriate time-dependent one-body Hamiltonian

$$\hat{H}(t) = \hat{H}_0 - 2\sum_i \varepsilon_i - \mathcal{E}(t)\hat{z}. \tag{42}$$

The one-body operator $\hat{H}_0$ describes the motion of independent electrons in a (mean-field) potential $V_{\mathrm{SAE}}(\mathbf{x})$ [cf. Eq. (1)]. The time evolution of the coefficients in the TDCIS expansion of Eq. (6) is then given by Eq. (26) and

$$i\dot{\alpha}_i^a = (\varepsilon_a - \varepsilon_i)\alpha_i^a - \mathcal{E}(t)\left\{\sqrt{2}\alpha_0 z_{ai} + \sum_{a'} \alpha_i^{a'} z_{aa'} - \sum_{i'} \alpha_{i'}^a z_{i'i}\right\}. \tag{43}$$

As in the case of the exact time-dependent many-body Hamiltonian, it is possible to derive a set of coupled equations of motion for the time-dependent orbitals $|\chi_i, t\rangle$ defined in Eq. (30);

$$i\frac{\partial}{\partial t}|\chi_i,t\rangle = (\hat{H}_0 - \varepsilon_i)|\chi_i,t\rangle - \mathcal{E}(t)\hat{P}\hat{z}\{\alpha_0|\varphi_i\rangle + |\chi_i,t\rangle\} + \mathcal{E}(t)\sum_{i'} z_{i'i}|\chi_{i'},t\rangle. \tag{44}$$

Equation (35) remains unchanged.

In analogy to the s-SAE approach, we now consider the special case of a single active orbital (SAO), which we will refer to as $|\varphi_{\mathrm{SAO}}\rangle$. (Similarly, the orbital describing the excitation out of $|\varphi_{\mathrm{SAO}}\rangle$ is symbolized by $|\chi_{\mathrm{SAO}}, t\rangle$.) Typically, for strong-field applications, $|\varphi_{\mathrm{SAO}}\rangle$ is chosen as the energetically highest occupied orbital. In case of degeneracies (i.e., if there is not a single highest occupied orbital), additional criteria have to be applied (see, for example, Ref. [57]). In the SAO approximation, single excitations out of $|\varphi_{\mathrm{SAO}}\rangle$ are allowed, but all other orbitals $|\varphi_i\rangle$ remain doubly occupied throughout. This makes it possible to combine the information contained in $\alpha_0(t)$ [Eq. (35)] and $|\chi_{\mathrm{SAO}}, t\rangle$ [Eq. (44)] into a single orbital

$$|\psi,t\rangle \coloneqq \alpha_0(t)|\varphi_{\mathrm{SAO}}\rangle + |\chi_{\mathrm{SAO}},t\rangle. \tag{45}$$

Choosing the energy $\varepsilon_{\mathrm{SAO}}$ of $|\varphi_{\mathrm{SAO}}\rangle$ as the origin of the one-electron energy scale, the effective one-electron Schrödinger equation satisfied by $|\psi, t\rangle$ is found to be

$$i\frac{\partial}{\partial t}|\psi,t\rangle = \left\{\frac{\hat{p}^2}{2} + \hat{V}_{\mathrm{SAE}}\right\}|\psi,t\rangle - \mathcal{E}(t)\{\hat{P} + 2|\varphi_{\mathrm{SAO}}\rangle\langle\varphi_{\mathrm{SAO}}|\}\hat{z}|\psi,t\rangle. \tag{46}$$

Here, $\hat{\mathbf{p}}$ is the electron momentum operator. The projection operator $\hat{P}$ is defined in Eq. (32).

Even when it is recognized within the s-SAE approach that the effective one-electron wave function must remain orthogonal to all occupied orbitals except $|\varphi_{\mathrm{SAO}}\rangle$, the factor of 2 (instead of 1) multiplying the projection operator $|\varphi_{\mathrm{SAO}}\rangle\langle\varphi_{\mathrm{SAO}}|$ in Eq. (46) cannot be reproduced. The origin of this factor can be traced back to the determinantal spin-singlet ansatz made for the many-electron wave packet in Eqs. (6) and (7). We therefore refer to Eq. (46) as the d-SAE approximation. Note that the time evolution of the effective one-electron wave function $|\psi, t\rangle$ is nonunitary. The norm of the many-electron wave function $|\Psi, t\rangle$, however, is conserved.

Another difference of d-SAE from s-SAE is revealed when the expectation value, with respect to $|\Psi, t\rangle$, of a spin-independent one-body operator $\hat{D}$ [cf. Eq. (36)] is expressed in terms of the orbital $|\psi, t\rangle$;

$$\langle\Psi,t|\hat{D}|\Psi,t\rangle = 2\langle\psi,t|\hat{d}|\psi,t\rangle. \tag{47}$$

The factor of 2 in this equation can also not be understood if it is assumed that $\langle\Psi, t|\hat{D}|\Psi, t\rangle$ can be obtained from the dynamics of a single electron moving in an effective potential [cf. Eq. (2)].

Finally, we would like to emphasize that in contrast to the TDCIS method developed in Sec. II A, d-SAE is not an *ab initio* method. The d-SAE method, just like the s-SAE method, depends on the choice made for the potential $V_{\mathrm{SAE}}(\mathbf{x})$.

III. TWO-ELECTRON MODEL SYSTEM

To test the accuracy of the TDCIS and d-SAE approaches derived in Secs. II A and II B, we introduce a one-dimensional (1D) two-electron model system for helium interacting with a laser field. As a figure of merit, we choose the time-dependent dipole moment of the system. The lowered dimensionality of the model allows one to easily solve the time-dependent two-electron Schrödinger equation

$$i\frac{\partial}{\partial t}\Psi(x_1,x_2,t) = \hat{H}(t)\Psi(x_1,x_2,t) \tag{48}$$

numerically and, thus, to establish a benchmark for comparison. Related systems served already in the past to assess the

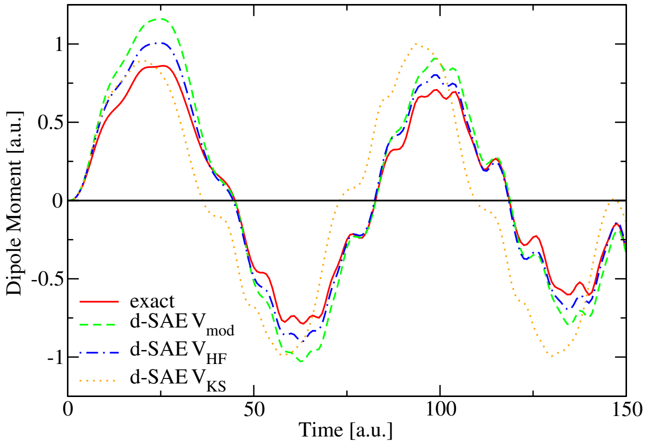

FIG. 1. (Color online) Comparison of the dipole moment of the exact 1D helium model (solid line) and the dipole moment calculated using the d-SAE approximation [Eqs. (46) and (47)]. The three different one-electron potentials V_{mod} (dashed line), V_{HF} (dashed-dotted line), and V_{KS} (dotted line) employed in the d-SAE calculation are explained in the text.

quality of various self-consistent-field approaches [38,39,58–62].

The two-particle Hamiltonian of the model system (in first quantization) is given by

$$\hat{H}(t) = \sum_{i=1,2}\left(\frac{p_i^2}{2} - \frac{2}{1+|x_i|} - \mathcal{E}(t)x_i\right) + \frac{1}{1+|x_1-x_2|}. \quad (49)$$

The Coulomb interaction is modeled by a singularity-free cusp potential [63], which allows the electrons to bypass each other. The laser electric field $\mathcal{E}(t)$ is chosen as a double-period sine wave of driving frequency ω;

$$\mathcal{E}(t) = \mathcal{E}_0 \sin(\omega t)\Theta(4\pi - \omega t), \quad t \geqslant 0. \quad (50)$$

The system starts from the ground state at $t=0$.

The Schrödinger equation (48) is discretized on an equidistant grid of grid spacing $\Delta x=0.147$. The simulation box size was chosen to be $|x_{\mathrm{max}}|=180$, which gives converged results for the considered laser parameters. An absorbing boundary was introduced at $x_{\mathrm{cut}}=\pm 150$ a.u. to avoid spurious reflections. The Schrödinger equation was propagated by means of the fourth order Runge-Kutta algorithm with a fixed time step of $\Delta t=0.0083$. Spatial integrals were solved using the trapezoidal rule.

The ground state of the two-particle Hamiltonian of Eq. (49) [$\mathcal{E}(t)=0$] was calculated by propagation in imaginary time; the ground-state energy of the 1D helium model was found to be $E_0^{\mathrm{He}}=-1.7181$. The ground-state energy of singly ionized 1D helium is $E_0^{\mathrm{He}^+}=-1.1402$ a.u. Hence, the ionization energy $I=E_0^{\mathrm{He}^+}-E_0^{\mathrm{He}}$ is 0.5779. The amplitude of the laser field was chosen as $\mathcal{E}_0=0.07$ a.u. at a driving frequency of $\omega=0.087$ a.u. (i.e., for single ionization of the 1D helium model at least seven photons are required).

For the s-SAE [Eq. (1)] and d-SAE [Eq. (46)] approaches, a one-particle potential $V_{\mathrm{SAE}}(x)$ must be selected. Figure 1 shows a comparison between the numerically exact dipole moment of the 1D helium model and d-SAE data obtained with three different one-particle potentials.

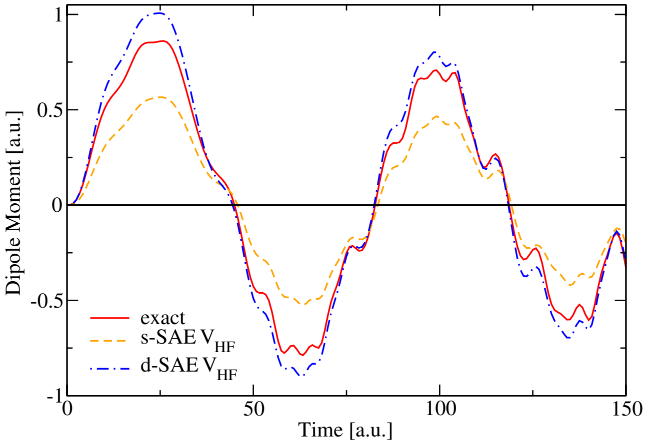

FIG. 2. (Color online) Time evolution of the dipole moment of the 1D helium model. Comparison of s-SAE [Eqs. (1) and (2)] and d-SAE [Eqs. (46) and (47)]. The one-particle potential used is V_{HF} [Eq. (52)].

The first effective one-particle potential $V_{\mathrm{mod}}(x)$ was chosen as an interpolation between the unscreened core potential $-2/(1+|x|)$ and the long-range $-1/(1+|x|)$ behavior of the electron-He$^+$ interaction potential;

$$V_{\mathrm{mod}}(x) = -\frac{1}{1+|x|}(1+e^{-a|x|}). \quad (51)$$

The parameter a was tuned so that the negative ground-state orbital energy in this potential equals the ionization energy I of the fully correlated 1D helium system. The second one-particle potential $V_{\mathrm{HF}}(x)$ is the converged Hartree-Fock potential for the Hartree-Fock ground-state orbital $|\varphi_0^{(\mathrm{HF})}\rangle$,

$$V_{\mathrm{HF}}(x) = -\frac{2}{1+|x|} + \int \frac{|\varphi_0^{(\mathrm{HF})}(x')|^2}{1+|x-x'|}dx'. \quad (52)$$

The Hartree-Fock ground-state orbital energy is $\varepsilon_0^{(\mathrm{HF})}=-0.5756$ a.u. The third one-particle potential is the effective Kohn-Sham potential $V_{\mathrm{KS}}(x)$ producing the exact ground-state density $n_0(x)$ of the fully interacting two-electron system, which can be easily constructed from the exact density [62,64] in the two-electron case considered;

$$V_{\mathrm{KS}}(x) = \frac{1}{4}\frac{n_0''}{n_0} - \frac{1}{8}\left(\frac{n_0'}{n_0}\right)^2 + \varepsilon_0^{(\mathrm{KS})}. \quad (53)$$

The effective Kohn-Sham ground-state orbital energy $\varepsilon_0^{(\mathrm{KS})}$ may be chosen such that $\lim_{x\to\pm\infty} V_{\mathrm{KS}}(x)=0$.

All potentials asymptotically approach $-1/(1+|x|)$. As illustrated in Fig. 1, the Hartree-Fock potential V_{HF} gives the best agreement with the exact result. The largest discrepancy is observed with the Kohn-Sham potential V_{KS}, where the dipole moment is noticeably out of phase with the exact solution.

In Fig. 2, we show a comparison of s-SAE and d-SAE, based on V_{HF}. d-SAE slightly overestimates the magnitude of

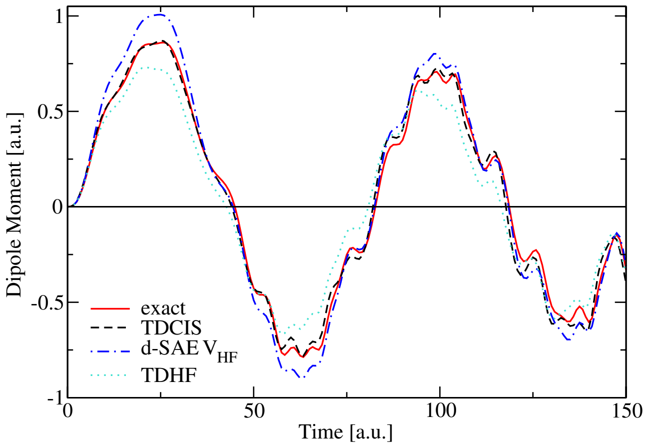

FIG. 3. (Color online) Comparison of the dipole moment of the exact 1D helium model, TDCIS, d-SAE (with V_{HF}), and TDHF. The TDCIS dipole moment is almost indistinguishable from the exact result.

the dipole moment, whereas s-SAE is seen to underestimate the magnitude of the dipole moment by a greater amount. This result suggests that the simple d-SAE approach, which requires essentially the same computational effort as s-SAE, is a cost-effective way to correct at least some of the shortcomings of s-SAE.

Even higher accuracy is obtained with the TDCIS orbital equations [Eqs. (33), (35), and (36)]. As a matter of fact, for the model system studied here, the TDCIS dipole moment is almost indistinguishable from the exact one. This is shown in Fig. 3. The small differences between the exact dipole moment and the TDCIS result are due to doubly-excited configurations, which are not included in TDCIS (see Sec. II). Note that the TDCIS dipole moment is a pure *ab initio* result: In a first step, a restricted Hartree-Fock calculation was performed for the laser-unperturbed atomic ground state. The calculated Hartree-Fock ground-state orbital energy $\varepsilon_0^{(\mathrm{HF})}$ was then inserted into Eq. (33); the Hartree-Fock ground-state orbital $|\varphi_0^{(\mathrm{HF})}\rangle$ was used to construct the operators $\hat{H}_0$, $\hat{J}_{00}$, and $\hat{K}_{00}$ [cf. Eq. (33)].

Also plotted in Fig. 3 is the result of a restricted TDHF calculation. In the case of two electrons in a spin-singlet state, the equation of motion for the doubly occupied TDHF orbital $|\varphi_{\mathrm{TDHF}},t\rangle$ is given by

$$i\frac{\partial}{\partial t}\varphi_{\mathrm{TDHF}}(x,t)=\left[-\frac{1}{2}\frac{\partial^2}{\partial x^2}-\frac{2}{1+|x|}+\int\frac{|\varphi_{\mathrm{TDHF}}(x',t)|^2}{1+|x-x'|}dx' - \mathcal{E}(t)x\right]\varphi_{\mathrm{TDHF}}(x,t) \tag{54}$$

with the initial condition $|\varphi_{\mathrm{TDHF}},t=0\rangle=|\varphi_0^{(\mathrm{HF})}\rangle$. (For the spin-singlet system starting from the ground state, the TDHF equations are equivalent to the time-dependent Kohn-Sham equations in the self-interaction corrected version of the exchange-only adiabatic local density approximation [65].) As can be seen in Fig. 3, the TDHF approximation underestimates the magnitude of the dipole moment. The accuracy is comparable to that achieved with the simple d-SAE method.

We would like to mention that simply replacing $\varphi_{\mathrm{TDHF}}(x',t)$ in the electron-electron interaction term of Eq. (54) with $\varphi_0^{(\mathrm{HF})}(x')$ [35] is equivalent to s-SAE using V_{HF}, except for the fact that, in contrast to Eq. (2), the dipole moment is given by $\langle x\rangle=2\langle\varphi_{\mathrm{TDHF}},t|x|\varphi_{\mathrm{TDHF}},t\rangle$ [cf. Eq. (47)]. The magnitude of the resulting dipole moment (not shown) exceeds the magnitude of the d-SAE dipole moment noticeably. Also note that linearizing Eq. (54) by assuming that $|\varphi_{\mathrm{TDHF}},t\rangle$ differs only little from $|\varphi_0^{(\mathrm{HF})}\rangle$, as suggested in Ref. [35], is not equivalent to the TDCIS equations (33) and (35).

IV. CONCLUSIONS

In this paper, we have suggested configuration-interaction-based techniques—d-SAE and TDCIS—for treating the electronic dynamics of an initially closed-shell atom or molecule in a strong optical laser field. The methods are applicable to problems where it is sufficient to focus on the excitation of at most one electron. The production of high-order harmonics is an example.

The d-SAE method is a single-active-electron approach in the sense that the associated equation of motion (46) describes the time evolution of an electron excited from one selected occupied orbital. It is derived, assuming a one-body Hamiltonian, from a many-body wave function [Eq. (6)] that preserves the spin symmetry. Channel couplings are not included. TDCIS improves on d-SAE through a systematic treatment of electron-electron interactions. In general, TDCIS involves the propagation of several coupled orbitals $|\chi_i\rangle$. The excited electron described by the TDCIS equations of motion (33) and (35) has a certain probability, given by the respective density-matrix element $\rho_{ii}^{(\mathrm{ion})}(t)$ [Eq. (39)], that its excitation is accompanied by the formation of a hole in the (initially doubly occupied) orbital $|\varphi_i\rangle$. Even if the laser field couples primarily to the most weakly bound orbital, electron-electron interactions may cause (virtual) excitations from deeper lying orbitals. The d-SAE method is a much simpler and less accurate method, but our calculations indicate that it is clearly preferable over the s-SAE method. In a recent investigation of the role of many-electron dynamics in HHG [22], we employed the d-SAE method.

The success of the TDCIS method in our 1D helium model calculation is encouraging. Since TDCIS is more accurate than, e.g., TDHF, at essentially the same computational cost, we believe that the time-dependent orbital formulation of TDCIS could become a useful tool for *ab initio* calculations on atoms and molecules exposed to a strong laser pulse. In particular, if such phenomena as HHG are to be experimentally exploited to study the electronic structure of molecules, guidance by reliable *ab initio* calculations seems crucial. A practical implementation of TDCIS in the molecular case in three dimensions might benefit from combining a Gaussian basis set, which is the standard in molecular quantum chemistry (see, for example, Ref. [66]), with a more flexible grid basis, e.g., a finite-element basis (see, for example, Ref. [67]). The Gaussian basis set would be used to represent the $|\varphi_i\rangle$. It could also be used to represent the $|\chi_i\rangle$ in the vicinity of the atomic nuclei. The purpose of the grid basis would be to describe the dynamics of the $|\chi_i\rangle$, primarily in the region outside the molecule. A similar idea was proposed in Ref. [68] for the treatment of electron-molecule collisions.

ACKNOWLEDGMENTS

N.R. would like to thank Joachim Burgdörfer for providing access to the computational resources of his group. N.R. and R.S. were supported by the Office of Basic Energy Sciences, Office of Science, U.S. Department of Energy, under Contract No. W-31-109-ENG-38. A.G. gratefully acknowledges support by AFOSR under Grant No. FA9550-04-1-0011.

[1] A. McPherson, G. Gibson, H. Jara, U. Johann, T. S. Luk, I. A. McIntyre, K. Boyer, and C. K. Rhodes, J. Opt. Soc. Am. B **4**, 595 (1987).
[2] M. Ferray, A. L'Huillier, X. F. Li, L. A. Lompre, G. Mainfray, and C. Manus, J. Phys. B **21**, L31 (1988).
[3] T. Brabec and F. Krausz, Rev. Mod. Phys. **72**, 545 (2000).
[4] Ch. Spielmann, N. H. Burnett, S. Santania, R. Koppitsch, M. Schnürer, C. Kan, M. Lenzner, P. Wobrauschek, and F. Krausz, Science **278**, 661 (1997).
[5] Z. Chang, A. Rundquist, H. Wang, M. M. Murnane, and H. C. Kapteyn, Phys. Rev. Lett. **79**, 2967 (1997).
[6] E. A. Gibson, A. Paul, N. Wagner, R. Tobey, D. Gaudiosi, S. Backus, I. P. Christov, A. Aquila, E. M. Gullikson, D. T. Attwood, M. M. Murnane, and H. C. Kapteyn, Science **302**, 95 (2003).
[7] E. A. Gibson, A. Paul, N. Wagner, R. Tobey, S. Backus, I. P. Christov, M. M. Murnane, and H. C. Kapteyn, Phys. Rev. Lett. **92**, 033001 (2004).
[8] J. Seres, E. Seres, A. J. Verhoef, G. Tempea, C. Streli, P. Wobrauschek, V. Yakovlev, A. Scrinzi, C. Spielmann, and F. Krausz, Nature (London) **433**, 596 (2005).
[9] M. Hentschel, R. Kienberger, Ch. Spielmann, G. A. Reider, N. Milosevic, T. Brabec, P. Corkum, U. Heinzmann, M. Drescher, and F. Krausz, Nature (London) **414**, 509 (2001).
[10] P. Agostini and L. F. DiMauro, Rep. Prog. Phys. **67**, 813 (2004).
[11] R. Velotta, N. Hay, M. B. Mason, M. Castillejo, and J. P. Marangos, Phys. Rev. Lett. **87**, 183901 (2001).
[12] H. Niikura, F. Légaré, R. Hasbani, A. D. Bandrauk, M. Yu. Ivanov, D. M. Villeneuve, and P. B. Corkum, Nature (London) **417**, 917 (2002).
[13] J. Itatani, J. Levesque, D. Zeidler, H. Niikura, H. Pépin, J. C. Kieffer, P. B. Corkum, and D. M. Villeneuve, Nature (London) **432**, 867 (2004).
[14] J. Itatani, D. Zeidler, J. Levesque, M. Spanner, D. M. Villeneuve, and P. B. Corkum, Phys. Rev. Lett. **94**, 123902 (2005).
[15] S. Baker, J. S. Robinson, C. A. Haworth, H. Teng, R. A. Smith, C. C. Chirila, M. Lein, J. W. G. Tisch, and J. P. Marangos, Science **312**, 424 (2006).
[16] P. B. Corkum, Phys. Rev. Lett. **71**, 1994 (1993).
[17] M. Lewenstein, Ph. Balcou, M. Yu. Ivanov, A. L'Huillier, and P. B. Corkum, Phys. Rev. A **49**, 2117 (1994).
[18] M. Yu. Ivanov, T. Brabec, and N. Burnett, Phys. Rev. A **54**, 742 (1996).
[19] N. Moiseyev and F. Weinhold, Phys. Rev. Lett. **78**, 2100 (1997).
[20] M. Kitzler, J. Zanghellini, Ch. Jungreuthmayer, M. Smits, A. Scrinzi, and T. Brabec, Phys. Rev. A **70**, 041401(R) (2004).
[21] R. Santra and A. Gordon, Phys. Rev. Lett. **96**, 073906 (2006).
[22] A. Gordon, F. X. Kärtner, N. Rohringer, and R. Santra, Phys. Rev. Lett. **96**, 223902 (2006).
[23] K. C. Kulander, Phys. Rev. A **38**, 778 (1988).
[24] J. Javanainen, J. H. Eberly, and Q. Su, Phys. Rev. A **38**, 3430 (1988).
[25] K. C. Kulander and B. W. Shore, Phys. Rev. Lett. **62**, 524 (1989).
[26] J. H. Eberly, Q. Su, and J. Javanainen, Phys. Rev. Lett. **62**, 881 (1989).
[27] W. Becker, S. Long, and J. K. McIver, Phys. Rev. A **41**, 4112 (1990).
[28] W. Becker, S. Long, and J. K. McIver, Phys. Rev. A **50**, 1540 (1994).
[29] N. H. Shon, A. Suda, and K. Midorikawa, Phys. Rev. A **62**, 023801 (2000).
[30] K. C. Kulander, Phys. Rev. A **36**, 2726 (1987).
[31] M. Lein, N. Hay, R. Velotta, J. P. Marangos, and P. L. Knight, Phys. Rev. Lett. **88**, 183903 (2002).
[32] X.-M. Tong and Shih-I Chu, Phys. Rev. A **57**, 452 (1998).
[33] Xi Chu and Shih-I Chu, Phys. Rev. A **63**, 023411 (2001).
[34] M. S. Pindzola, D. C. Griffin, and C. Bottcher, Phys. Rev. Lett. **66**, 2305 (1991).
[35] K. C. Kulander, K. J. Schafer, and J. L. Krause, in *Atoms in Intense Radiation Fields*, edited by M. Gavrila (Academic Press, New York, 1992).
[36] N. E. Dahlen and R. van Leeuwen, Phys. Rev. A **64**, 023405 (2001).
[37] V. Véniard, R. Taïeb, and A. Maquet, Laser Phys. **13**, 465 (2003).
[38] N. Rohringer, S. Peter, and J. Burgdörfer, Phys. Rev. A (to be published).
[39] J. Zanghellini, M. Kitzler, T. Brabec, and A. Scrinzi, J. Phys. B **37**, 763 (2004).
[40] M. Nest, T. Klamroth, and P. Saalfrank, J. Chem. Phys. **122**, 124102 (2005).
[41] A. Szabo and N. S. Ostlund, *Modern Quantum Chemistry* (Dover, Mineola, NY, 1996).
[42] J. B. Foresman, M. Head-Gordon, J. A. Pople, and M. J. Frisch, J. Phys. Chem. **96**, 135 (1992).
[43] A. Dreuw and M. Head-Gordon, Chem. Rev. (Washington, D.C.) **105**, 4009 (2005).
[44] M. Nest and T. Klamroth, Phys. Rev. A **72**, 012710 (2005).
[45] T. Klamroth, J. Chem. Phys. **124**, 144310 (2006).
[46] A. L. Fetter and J. D. Walecka, *Quantum Theory of Many-Particle Systems* (McGraw-Hill, Boston, 1971).

[47] A. A. Abrikosov, L. P. Gorkov, and I. E. Dzyaloshinski, *Methods of Quantum Field Theory in Statistical Physics* (Dover, New York, 1975).

[48] T. Koopmans, Physica (Amsterdam) **1**, 104 (1933).

[49] L. S. Cederbaum, G. Hohlneicher, and W. von Niessen, Chem. Phys. Lett. **18**, 503 (1973).

[50] D. P. Chong, F. G. Herring, and D. McWilliams, J. Chem. Phys. **61**, 78 (1974).

[51] K. Blum, *Density Matrix Theory and Applications* (Plenum Press, New York, 1996).

[52] M. D. Feit and J. A. Fleck, Jr., J. Chem. Phys. **78**, 301 (1983).

[53] M. H. Beck, A. Jäckle, G. A. Worth, and H.-D. Meyer, Phys. Rep. **324**, 1 (2000).

[54] M. R. Wall and D. Neuhauser, J. Chem. Phys. **102**, 8011 (1995).

[55] V. A. Mandelshtam and H. S. Taylor, Phys. Rev. Lett. **78**, 3274 (1997).

[56] C. Leforestier, R. H. Bisseling, C. Cerjan, M. D. Feit, R. Friesner, A. Guldberg, A. Hammerich, G. Jolicard, W. Karrlein, H.-D. Meyer, N. Lipkin, O. Roncero, and R. Kosloff, J. Comput. Phys. **94**, 59 (1991).

[57] K. C. Kulander and T. N. Rescigno, Comput. Phys. Commun. **63**, 523 (1991).

[58] R. Grobe and J. H. Eberly, Phys. Rev. A **48**, 4664 (1993).

[59] D. Bauer, Phys. Rev. A **56**, 3028 (1997).

[60] M. S. Pindzola, F. Robicheaux, and P. Gavras, Phys. Rev. A **55**, 1307 (1997).

[61] D. G. Lappas and R. van Leeuwen, J. Phys. B **31**, L249 (1998).

[62] M. Lein and S. Kümmel, Phys. Rev. Lett. **94**, 143003 (2005).

[63] A. Gordon, R. Santra, and F. X. Kärtner, Phys. Rev. A **72**, 063411 (2005).

[64] I. D'Amico and G. Vignale, Phys. Rev. B **59**, 7876 (1999).

[65] J. P. Perdew and A. Zunger, Phys. Rev. B **23**, 5048 (1982).

[66] R. Santra and L. S. Cederbaum, J. Chem. Phys. **115**, 6853 (2001).

[67] S. Tonzani and C. H. Greene, J. Chem. Phys. **122**, 014111 (2005).

[68] T. N. Rescigno, D. A. Horner, F. L. Yip, and C. W. McCurdy, Phys. Rev. A **72**, 052709 (2005).